Journal of Computer Science

Research Article

Chronic Lung Disease Identification in Chest CT Scans Through Hybrid Deep Transfer Learning Framework

Garima Jain, Amit Kumar Goel and Rahul Kumar

Faculty of Computing and Informatics, Sir Padampat Singhania University, Udaipur, India

Article history
Received: 25-04-2026
Revised: 13-07-2026
Accepted: 29-07-2026

Corresponding Author:
Garima Jain
Faculty of Computing and Informatics, Sir Padampat Singhania University, Udaipur, India
Email: garima.phd2023@spsu.ac.in

Abstract: Accurate and timely diagnosis is essential for successful treatment of chronic pulmonary conditions, particularly lung tumours. To capture more complicated pathological characteristics, diagnostic algorithms based on current data sets are restricted to using older databases and single branch systems. This research introduces a new solution: A hybrid deep learning model applied to a recently released quantitative database of CT scans of the chest. This method combines a pre-trained ResNet50 backbone with a Multi-Layer Perceptron (MLP) to merge high level spatial properties with statistically determined measures (mean intensity, standard deviation and entropy). In addition, the two branch fusion handles extremely mechanical diagnosis and global spatial characteristics of the images, facilitating the classification of adenocarcinoma, large cell carcinoma, squamous cell carcinoma and normal tissue. After extensive preprocessing and data augmentation, our framework reached a reliable training accuracy of 94.00% and a testing accuracy of 88.0%. While this represents the greater benefit of incorporating both deep spatial learning into statistical measures, this specific architecture was purposely optimized for functioning within standard computational systems that are restricted to a limited amount of CPU and memory resources. As such, this work serves as a resource-efficient proof-of-concept. This framework provides a foundation for a potential computer-aided diagnostic support system that could assist radiologists in identifying chronic lung conditions.

Keywords: Hybrid Deep Learning, Chest CT Imaging, ResNet50-MLP, Lung Cancer Classification, Feature Fusion, Computer Aided Diagnosis (CAD)

Introduction

The most important thing to look for in patients with lung cancer or other chronic lung diseases is an early, accurate, and reliable diagnosis; diagnosing patients with lung cancers or chronic lung diseases early and accurately can significantly improve each patient's chances of survival (Davri et al., 2023; Ichahane et al., 2026; Purohit et al., 2025). Computed Tomography (CT) has proven to be one of the most efficient means of diagnosing lung diseases because of its high resolution and ability to visualize the lung anatomy very accurately (Ramasamy and Doshi, 2022). However, patients who receive their CT scans are often interpreted by the radiologists on a manual basis, making it time-consuming and subjective when determining abnormalities in the lungs, and there are considerable differences between the accuracy of how one radiologist interprets a CT scan and how another radiologist interprets the same CT scan (Huang et al., 2025; Sun et al., 2022). This has created an increased reliance on CAD technology in clinical decision-making. In recent years, deep learning has gained noticeable success in improving computerized systems for the automated detection and classification of lung cancers from CT (Javed et al., 2024; Khan et al., 2026; Şerbănescu et al., 2020). Recent studies have shown that the use of transfer learning and CNN for lung cancer diagnosis using CT images has been successful in classifying CT images as having an abnormality with an accuracy of between 87 and 92% using multiple types of neural network architectures, including but not limited to transformer-based architectures. Attention models are being

developed that enable refinement or better localization of features based on assigning attention weights to the most salient areas in CT images; however, these have been largely reliant on using deep spatial features alone (UrRehman et al., 2024). While they do provide good results compared to conventional Machine Learning Techniques (MLT), their output is limited because of variable datasets, a limited number of training samples, and single-modality dataset dependencies (Gote et al., 2025; Sui et al., 2025).

Most of the current deep learning algorithms for medical imaging only have a single branch of processing power. Consequently, they are limited in their ability to learn complete format feature representations (Abdulqader et al., 2025). The hybrid and multi-objective architectures that combine multiple types of tasks, such as detecting objects, classifying objects, and localizing objects, prioritize accurate detection over accurate classifications between multiple classes (Hosny et al., 2025; Jain et al., 2023). Thus, these architectures fall short when a high level of precision is required. Additionally, others have also shown that combining handcrafted features with deep learning will yield marginal increases in accuracy. These models are typically restricted by their inadequate representation of features and their limited ability to generalize (Kamala and Mohan, 2025). Detection-based methods can very accurately locate tumor regions, but they are not conducive to very precise classifications between multiple classes and can only be utilized in the diagnostic path when determining if a tumor is present and in an earlier stage of detection (Choudhury et al., 2025; Nahmatwlla and Ali, 2026).

There are still various issues with the current models that are present, such as low accuracy rates, high computational costs, and not being very robust with regard to different data sets. The models available lack efficiency in their integration of features and therefore, are unable to efficiently use available information within CT images which makes models less clinically robust and less able to scale effectively. The proposed hybrid model achieves an overall classification accuracy of 94% and has the potential to serve as an effective computer-aided diagnostic tool for predicting and classifying chronic lung disease.

Figure 1 presents the graphical abstract of the proposed hybrid deep learning framework for chronic lung disease prediction using chest CT-scan images.

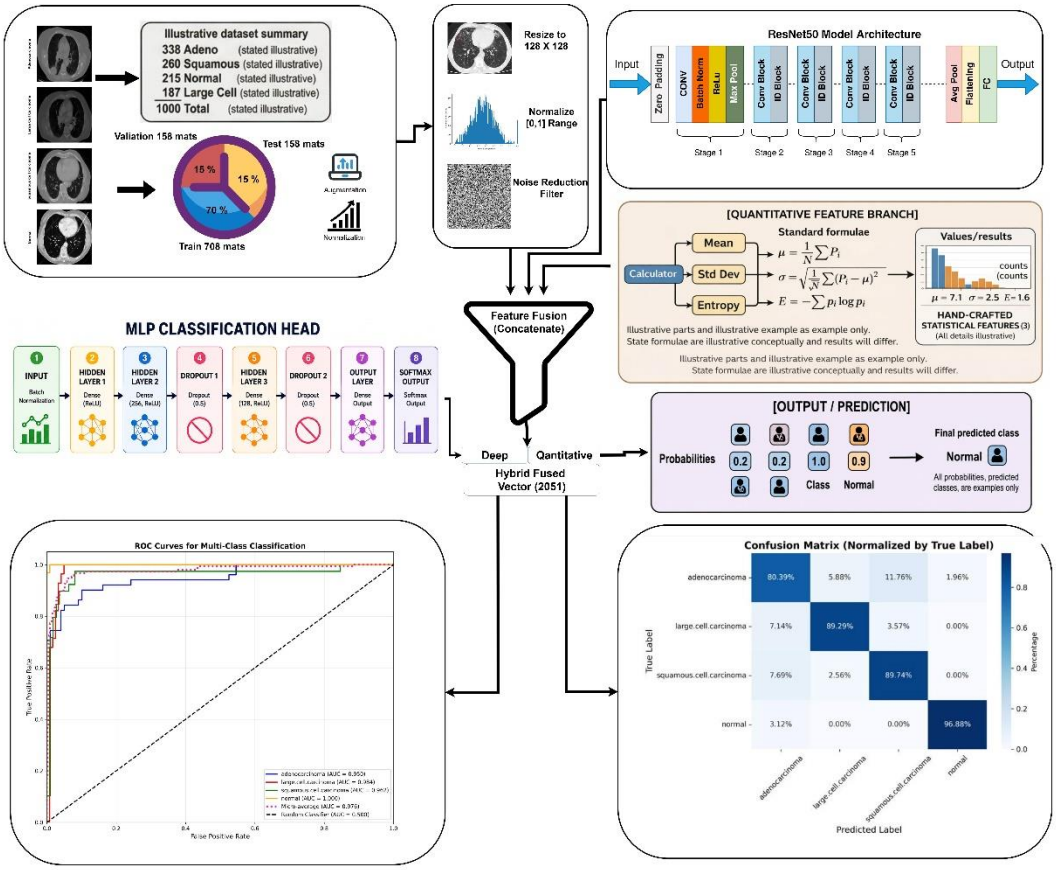

Fig. 1: Graphical Abstract for Hybrid DL models for Chronic Lungs Disease Prediction

It shows the complete end-to-end computational pipeline beginning with dataset preparation, class distribution analysis, and stratified train validation test splitting of the multi-class CT dataset. The workflow then demonstrates the image preprocessing stage, including resizing, normalization, augmentation, and noise reduction operations performed to improve image consistency and model generalization. Following pre-processing, the architecture adopts a dual-branch feature extraction strategy in which deep spatial representations are extracted using a fine-tuned ResNet50 backbone while parallel handcrafted quantitative descriptors, including mean intensity, standard deviation, and entropy, are computed through the statistical feature branch. Both representations are subsequently fused through feature concatenation to generate a unified 2051 - dimensional hybrid feature vector. The fused representation is then processed through the MLP classification head to produce multi-class diagnostic predictions for adenocarcinoma, squamous cell carcinoma, large cell carcinoma, and normal lung tissue. In addition to illustrating the proposed architecture, the graphical abstract also summarizes the model evaluation process through ROC curve analysis, confusion matrix visualization, and probability -based prediction outputs, thereby highlighting the framework's interpretability, robustness, and suitability for deployment in resource-constrained CAD environments.

Our hybrid deep learning model is identified as a new type of model with strong benefits in terms of being robust, having computationally efficient methods of defining features from a set of images, and successfully combining deep spatial feature extraction and quantitative statistical descriptors. The overall goal of this paper is to enhance the capabilities of early detection in patients with chronic lung diseases and to create multi-class diagnostic models to improve clinical outcomes. This section will present an overview of previous research and present the rationale for this project.

Literature Review

Faizi et al. (2025) presented a deep learning model based on transformer architecture directly from CT scan images to classify lung cancer using the images from LUNA16 dataset. Their model employs sophisticated attention-based mechanisms to effectively grasp intricate spatial relationships embedded in the images, yielding a classification accuracy close to 87.94%. The crystal-clear architecture atomizes back to an influential study imposed on peeling CNN models of visual features that a transformer can lead their individual teeth for the future of earth. Nonetheless, the model does not add complementary statistical or handcrafted features and is purely based on deep learning features. This restriction leads to moderate accuracy and limits the model's ability to generalise across varying dataset types as well as subtle pathological variations, especially in cases of multi-class classification.

Shatnawi et al. (2025) proposed a neural network-based deep learning approach involving multiple convolutional neural network architectures, including ConvNeXt and ResNet, for lung cancer classification using CT scan datasets. The model uses transfer learning and preprocessing methods to create a classifier that can predict backorders and attain 100% accuracy. Their work shows the efficiency of typical CNN architectures at extracting discriminative features from medical images. This method is somewhat limited due to their dependency on single - modality deep features and the lack of complementary statistical information. Consequently, the model becomes more challenging to distinguish between visually similar lung cancer subtypes that restrict its robustness for clinical applications in a more generalized manner.

Abdulqader et al. (2025) provided a multi-objective hybrid deep learning framework for detection, classification and localization with CT scan images. These employ YOLO-based architectures to boost detection accuracy and increase diagnostic rate by localizing potential lung regions. Although effective for tumor region identification, this technique is targeted primarily towards detection and not detailed multi-class classification. This results in lack of robustness for differentiating between the different subtypes of lung cancer, and does not provide comprehensive classification outputs, limiting its applicability in complete diagnostic systems.

Kamala and Mohan (2025) proposed a hybrid AI framework that integrates deep learning characteristics with handcrafted feature extraction methods to detect lung cancer in CT images. The model functions reasonably well (accuracy 97.2%), suggesting that integrating certain features may improve classification. Nevertheless, the method is limited by incomplete feature extraction and lack of generalization due to its reliance on hand-engineered features. In addition, the hybridization is not optimized and does not have an effective feature fusion module that can fully exploit complementary information from CT images.

Choudhury et al. (2025) introduced a CNN-based classification model using transfer learning models like VGG16 and ResNet50 on the IQ-OTH/NCCD CT dataset. The proposed study shows that transfer learning as a process to improve classification performance, yielding around 98.7% accuracy. Their work illustrates the significance of utilizing pretrained models in employing medical image processing. But the model only relies on deep convolutional features and does not integrate hybrid features. This limitation reduces its ability to capture global statistical patterns and contextual information, thereby affecting robustness and generalization across diverse datasets.

Huang et al. (2025) presented a deep learning model using transfer learning and an attention mechanism in lung cancer classification from CT scan images. The model also enhances feature localization and interpretability via attention layers, but only achieves a moderate accuracy of

around 90.16%. Authors also describe a model that borrows from this format, but still is constrained by being fully image-feature based; whilst the approach makes the original model much better at attending to salient spatial features, it's clear that there are some limitations due to it being just image-features! The inability to integrate statistical features limits the model's ability to seize global properties, thus leading to moderate generalizability.

Inbasakaran and Ruth (2025), they created a classification model based on Convolutional Neural Networks (CNNs) that used IQ-OTH/CCD dataset containing about 1190 CT images. They attempted to improve their model's performance via data augmentation techniques, resulting in accuracies of 94%. The model is limited by having a quite small size dataset, which limits generalizability across a wide range of different clinical conditions. A second limitation associated with their model is that there is no hybrid features used to enhance the ability to extract global characteristics from the images.

UrRehman et al. (2024) proposed a multi-attention CNN (dual attention) model for detecting and classifying lung cancer from CT scan images. Attention Mechanisms: By integrating attention mechanisms into the model, it improves the focus on relevant areas within lung images, leading to more effective feature localization and interpretability. The best performance achieved by the model was found to be between 94.40% accuracy, thus showing that there is a boost when using attention for medical imaging tasks. Although these enhancements overcome some of the negatives of spatial structures, this method is still reliant on exponential and spatial characteristics. Moreover, the high computational requirements imposed by attention-based mechanisms render its use less practical for implementation in time-sensitive or resource-limited bedside clinical setting.

Table 1 describes the methodologies, datasets, and performance metrics of recent deep learning frameworks applied to lung cancer classification. The comparative analysis highlights a prevalent performance plateau between 87% and 100% accuracy, while emphasizing critical research gaps such as the over-reliance on single-modality features and the absence of robust statistical integration.

Research Gap

Through a thorough examination of published research findings, clear limitations were found in regard to existing CADs of chronic lung diseases which highlight an urgent need for the proposed architecture. The key gaps between current techniques can be categorized into:

1) Data set limitations
2) Limitations within the techniques of the architecture for CAD systems
3) Achieving a limit on multi-class predictive accuracy

The majority of current methodologies depend upon older, highly overused, or small datasets of images of input data for the training of a Deep Learning Model. Training of a Deep Learning Model on older, historical data prevents the models from being clinically relevant and allows them to create valid output to work with low-quality images.

To date, the latest studies indicate a continuing trend of high reliance on single-modality, unidirectional architectures. While vision transformers can be highly effective for extracting complex spatial hierarchies and localized abnormalities, they are unable to capture much larger macroscopic characteristics of tissue (Shafi and Chinnappan, 2024; Soni and Rai, 2023). The chronic lung carcinoma exhibits heterogeneous differences in tissue density and structural randomness. For example, multidimensional framework approaches (Bhattacharjya et al., 2025) tend to give little emphasis to the difficult task of detecting subtypes such as adenocarcinoma or squamous cell carcinoma, which appear similar (Khan and Aleem, 2025). Therefore, the limits imposed by these architectures and datasets have created saturation points in classification performance with recent classification accuracies approaching 87% and continuing to error between 87% and 93%. A multi-branch hybrid approach that takes advantage of highly quantitative, high-resolution CT dataset and that fuses the benefits of deep spatial feature extraction with the application of handcrafted statistical descriptors could break the generalization limitations of networks that rely solely on images. In particular, Shatnawi et al. (2025), who utilized the same chest CT dataset from Kaggle as the present investigation, reported an accuracy score of 100% on their testing data using innovative CNN architectures and image enhancement techniques. However, the extremely high accuracy achieved on a small dataset that has been repeatedly accessed may suggest potential problems with overfitting and very little ability to generalise to real-world scenarios. Additionally, they predominantly relied on spatial features of a deep CNN without integrating utilising either statistical descriptors or hybrid combinations of different features.

For this reason, there is an ongoing need for a more general, interpretable, and computationally efficient hybrid framework to combine both deep spatial representation and handcrafted statistical descriptors into a single diagnostic pipeline. An effective multi-branch architecture, where transfer-learning based spatial feature extraction is used along with quantitative descriptors, such as mean intensity, standard deviation, and Shannon entropy, can simultaneously capture localized structural abnormalities and global characteristics of the tissues being analysed. The proposed framework seeks to fill the gaps left by purely image-drive architectures and create a better, more trustworthy, and clinically acceptable Computer-Assisted Diagnosis (CAD) system for predicting and classifying chronic lung disease through feature fusion, explainable AI (XAI) mechanisms, entropy-guided tissue analysis, and balanced multiclass prediction.

Table 1: Literature Review

Author(s)	Dataset	Dataset Size	Model	Methodology	Accuracy	Contribution	Research Gap
(Baqir et al.,	Custom Lung CT	LC25000	Lightweigh t CNN	lightweight model,	96%	Achieves accuracy with significantly lower computational cost.	Not applicable for large models, not focus on clinical
2026)	(Multi-class)	1000 images	CNN (ConvNeXt	MiniConvNet	100%	Enhances classification using multiple architectures	Single-modality; no statistical feature integration
(Shatnawi et al.,	Kaggle CT	888 CT scans	ResNet)	Transfer learning with multiple CNN models	87.94%	Improves	Moderate accuracy; lacks hybrid feature fusion
2025)	Dataset	1608 images	Transforme r-based	Deep feature extraction using advanced DL architecture	96.26%	classification	Focus on detection; weak multi-class classification
(Faizi et al.,	LUNA16 (CT)	300 images	DL	Detection + classification + localization	97.20%	compared to CNN baselines	Incomplete feature extraction; lower accuracy
2025)	CT Dataset	1097 images	Hybrid DL (YOLObas ed)	Combines deep + manual features	98.70%	Multi-task learning improves detection	Limited robustness; lacks hybrid feature fusion
(Abdulqad er et al., 2025)	IQ-OTH/NC CD		Hybrid	Comparative CNN-		Attempts to feature integration	
(Kamala and	IQ-OTH/NC CD		DL(Mobile Net) + handcrafted (GLCM and SIFT)	based classification		Demonstrates effectiveness of transfer learning	
Mohan, 2025) (Choudhu ry et al., 2025)	CT Dataset		CNN (VGG16, ResNet50)	5			
(Huang et al., 2025)	CT Scan Dataset	1000 images	CNN + ResNet50V 2	Transfer learning with attention mechanism	90.16%	Improves feature localization and interpretability	No statistical features; moderate generalization
(Inbasakar an and Ruth, 2025)	IQ-OTH/NC CD	1190 images	CNN	CNN with augmentation & optimization	94%	Improves classification on small dataset	Small dataset; poor generalization
(UrRehman et al., 2024)	LUNA 16 Data Set	1351	CNN	Attention-based feature extraction	94.40%	Improves focus on relevant lung regions	High complexity; still single-branch architecture

Proposed Framework

The research will use a dataset1 of a repository dedicated to pulmonary oncology research and associated imaging. The overall dataset comprises a total of 1,000 high-quality CT Scan images that are created using image processing technologies.

Raw Data Attribute and Class Description – CT Slice Image Types: The raw data consists of a series of 2-dimensional CT Scan slices taken from various angles of patients and presented in either JPEG or PNG format. The dataset is separated into four categories based on clinical descriptions of the patient's pulmonary condition. In Adenocarcinoma, there is A Non-Small Cell Lung Cancer (NSCLC), which means that it originated in the glandular cells located in the outer areas of the lungs (Tone et al., 2025; Zaernia et al., 2024). There are 338 images currently available to view. The second type of lung squamous cell carcinoma, which means that it normally occurs in the central parts of the lungs (in the bronchi),

and has a significant association with a history of use to tobacco products (Córdoba et al., 2025; Raghu et al., 2024). There are 260 images currently available to view. The least common type of lung NSCLC and its cells grow rapidly in large cell carcinoma. This type of cancer may occur in any area of the lung and may spread easily from the lungs to other areas of the body (Sing et al., 2019). There are 187 images currently available to view. While in normal or healthy chest CT scans, a group of chest CT scans without any pathological findings or pulmonary abnormalities serves as a control group (Inbasakaran and Ruth, 2025; Mijwil et al., 2022). There are 215 images currently available to view.

Dividing and distributing the data: To ensure the model's ability to generalize in clinical settings, we performed a patient-level data split rather than an image-level split. This guarantees that images from the same patient are never shared across the training, validation, and testing sets, thereby preventing data leakage and ensuring an unbiased evaluation. To have the ability to generalise on data in clinical settings, a stratified partitioning was adopted for splitting the data images into training (70%), validation (15%) and testing (15%) subsets (whole dataset split). This approach ensures proportionate representation of the dataset's inherent class imbalance across all model-building phases. As a reference, the details of each split are found in Table 2.

Image based features selection: Processing pixels of data images directly provides a huge amount of computational overhead (e.g., RGB pixels of size 128×128×3 = 49,152 features/image) and increases risk of "curse of dimensionality". This is especially true since our dataset is small as only 1,000 images exist. Thus, we chose to extract from all raw features and instead create a carefully curated, highly compressed representation of all images (total 2,051 features/image).

Image Pre-processing and Data Augmentation

Prior to feature extraction, processing steps are applied to each image in the dataset to make the images uniform and improve model convergence. The first step is to look at both the distribution of CT scans across the dataset as well as the distribution of CT scans by lung disease category (Alsallal et al., 2025; Makimoto et al., 2025). The breakdown of how many total CT scans are in the dataset divided by how many CTs in each of the four categories of disease is provided in figure 2.

Images will be read using the OpenCV function for image processing and conversion procedures between the BGR and RGB color formats. All grayscale images will be replicated into three channels (RGB) to create the expected form of the input for the deep learning backbone. Different types of lung cancer (e.g. adenocarcinoma, squamous cell carcinoma, large cell carcinoma) will all be represented as part of the total sample set after being standardized and will therefore appear visually different from normal in Figure 3 (Forte et al., 2022; Kobylińska et al., 2022; Tone et al., 2025).

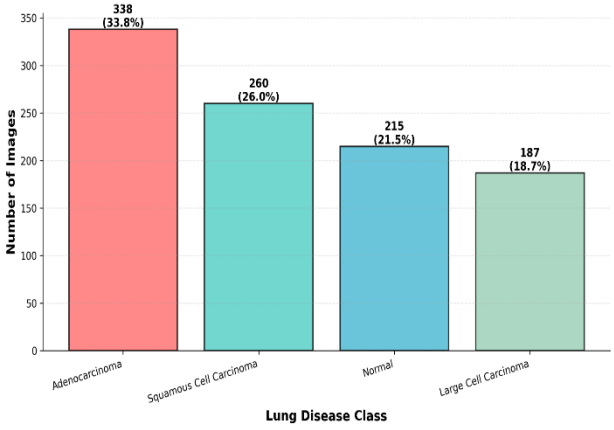

Fig. 2: Class distribution of chest CT-scan

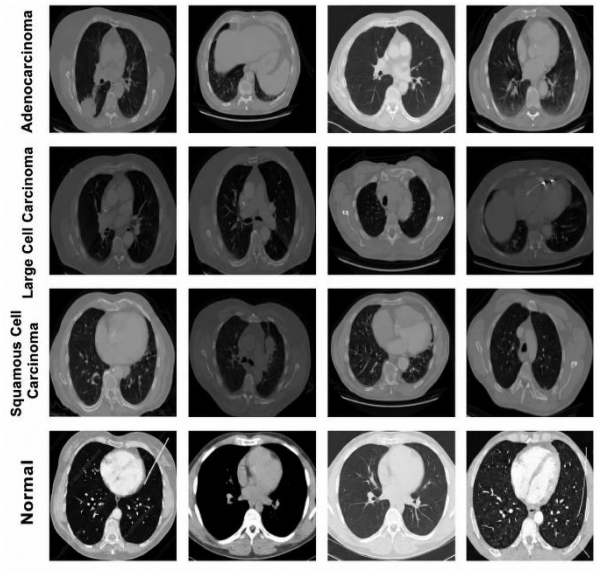

Fig. 3: Sample CT-scan images from each class illustrating visual variations

Table 2: Dataset Description

Class Label	Training	Validation	Test	Total	Percentage
Adenocarcinoma	236	51	51	338	33.8%
Squamous Cell Carcinoma	182	39	39	260	26.0%
Normal (Healthy)	151	32	32	215	21.5%
Large Cell Carcinoma	131	28	28	187	18.7%
Total Images	700	150	150	1000	100.0%

Normal scans are consistent in their means and have low entropy, but malignant scans cause differences. Adenocarcinomas exhibit local anomalies and ground-glass irregularities, which the ResNet50 spatial branch maps well through its convolutional layers; Squamous Cell Carcinomas exhibit chaotic internal textures and irregular margins, which produce spikes in standard deviation and entropy that the MLP statistical branch easily detects; Large Cell Carcinomas display large masses that alter the global mean intensity, which is another distinguishing property.

Resizing and Normalization of Images: CT images were adjusted to a size of 128 x 128 pixels using an area interpolation algorithm. This resizing and normalizing process preserved the structural characteristics of the images while keeping the computational complexity at a minimum. After the images were normalized, the pixel intensity values were set to the range of [0,1]. The result of resizing and normalizing resulted in all images in the dataset having the same dimensions and this is significant in making training faster.

Statistical Assessment of Pixel Intensity: To provide an understanding of the difference in class entries, we plotted a histogram (Figure 4) of the intensity of the pixels from each of the classes and we were able to see that the mean values of the pixels of the class of "normal" lung were approximately an order of magnitude larger than the mean pixel intensity of the other classes of cancers, which is indicative of a difference in the density and makeup of these two types of tissue. Based on the analysis above, we now have the basis for including the statistical descriptors of all pixel intensities in our proposed hybrid model.

Information Content and Noise Balance Analysis: To further evaluate the inherent image characteristics and validate the selected statistical features, a quality versus information trade-off analysis was conducted prior to model training. Figure 5 illustrates the relationship between the Signal-to-Noise Ratio (SNR) and the overall information content, measured as Shannon entropy in bits, across the dataset.

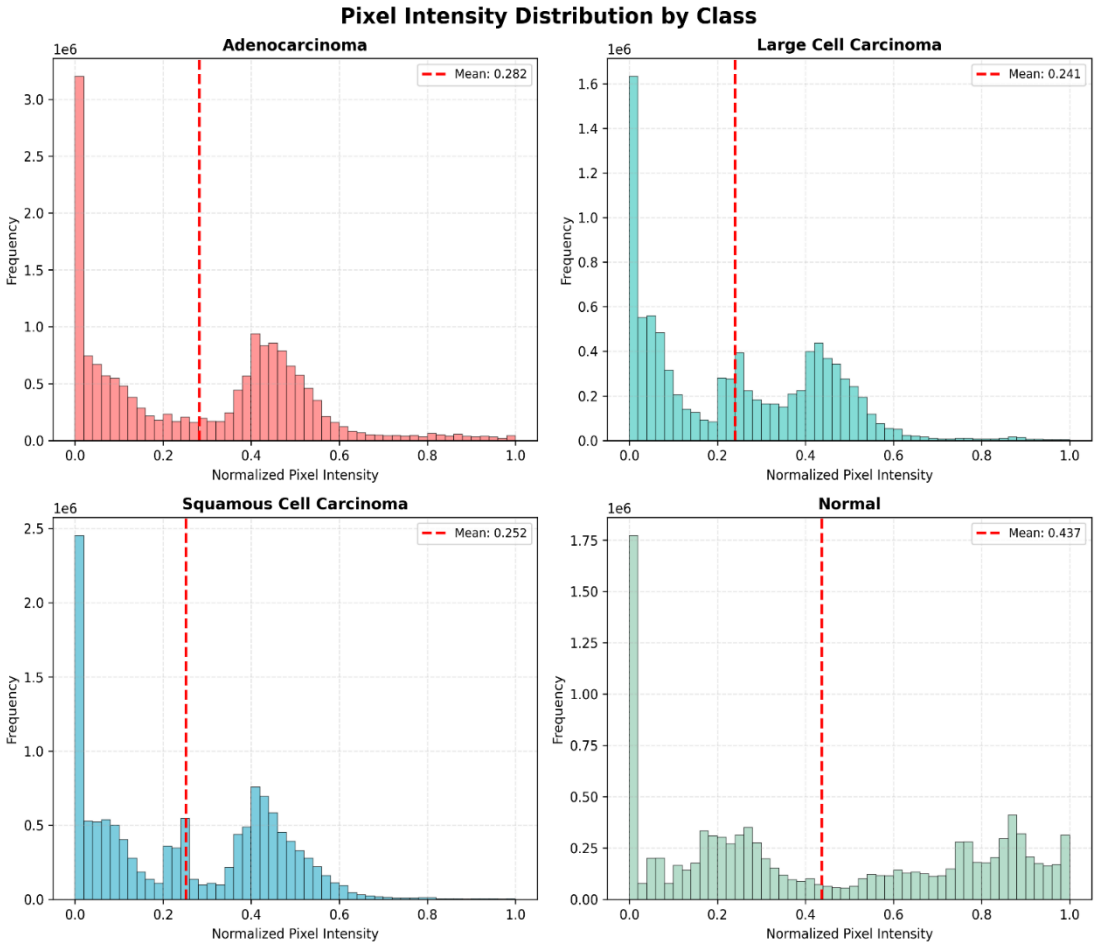

Fig. 4: Pixel intensity distribution across different lung diseases

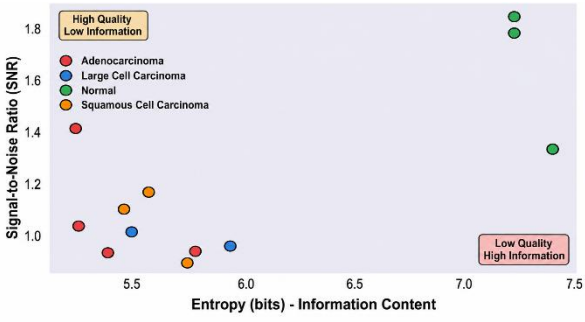

Fig. 5: Quality versus Information Trade-off Analysis

This analysis serves as a crucial noise balance assessment during the pre-processing phase. As observed in the scatter plot, 'Normal' lung tissue scans exhibit a distinctly higher entropy and SNR compared to the carcinoma classes, which predominantly cluster at lower entropy levels. This quantitative distinction highlights the structural degradation and homogeneity often found in cancerous tissues compared to the complex textures of healthy lungs, strongly justifying the explicit extraction of entropy as a core hand-crafted feature in our hybrid architecture.

Implementation and Workflow of Architecture

Figure 6 illustrates the complete end-to-end workflow of the proposed hybrid deep learning model for multiclass chronic lung disease prediction. The pipeline initiates with data preparation, where raw input CT scans are sorted, labeled, resized to identical dimensions, and normalized. To mitigate overfitting and enhance the model's ability to generalize to unseen data, spatial augmentation techniques including rotation, flipping, and zooming are applied. The pre-processed images then undergo parallel feature extraction: A ResNet50 backbone extracts deep spatial features while handcrafted statistical descriptors are generated simultaneously. These parallel outputs are subsequently concatenated into a unified hybrid vector and passed through a Multi-Layer Perceptron (MLP) classification head to generate precise multi-class predictions. Ultimately, this integration of spatial and statistical data ensures robust diagnostic accuracy, supported by comprehensive evaluative metrics such as confusion matrices and ROC curve analysis.

Algorithm 1 formalizes the computational optimization pipeline of the proposed hybrid architecture. The network performs parallel feature extraction at every training batch: While the fine-tuned ResNet50 backbone extracts a 2048-dimensional deep spatial vector, three statistical descriptors (mean, standard deviation, and entropy) are simultaneously computed by a separate quantitative branch of the network. The two representations are combined to create one unified 2051-dimensional hybrid vector, which is then classified by a Multi-Layer Perceptron (MLP) classification head, optimizing network weights iteratively via backpropagation using categorical cross-entropy loss and Adam optimizer.

Algorithm 1: High-Level End-to-End Diagnostic Workflow

Input: Raw Chest CT Scan Images with Multi-Class Labels
Output: Predicted Lung Disease Class (Adenocarcinoma, Large Cell Carcinoma, Squamous Cell Carcinoma, or Normal)

1: Data Preparation
  1.1 Ingest raw CT scans and assign multi-class labels.
  1.2 Perform stratified data splitting:
    70% Training, 15% Validation, and 15% Testing sets.

2: Pre-Processing
  2.1 Resize all images to 128 × 128 pixels.
  2.2 Normalize pixel intensities to [0,1].
  2.3 Apply data augmentation (rotation, flipping, zooming) on training data.

3: Parallel Feature Extraction
  3.1 Branch A – Deep Feature Extraction:
    F_deep ← ResNet50 (I_preprocessed)
      Extract 2048-dimensional spatial feature vector.
  3.2 Branch B – Statistical Feature Extraction:
    Compute μ, σ, H from image intensities
    F_stat ← [μ, σ, H]
      Form 3-dimensional statistical feature vector.

4: Feature Integration
  F_hybrid ← Concatenate(F_deep, F_stat)
    Form a unified 2051-dimensional hybrid feature vector.

5: Classification
  Pass hybrid vector through MLP (Dense → Dropout → Dense).
  Ŷ ← Softmax(Z)

6: Output Generation
  Predicted Class ← argmax(Ŷ)
  Return Predicted Class

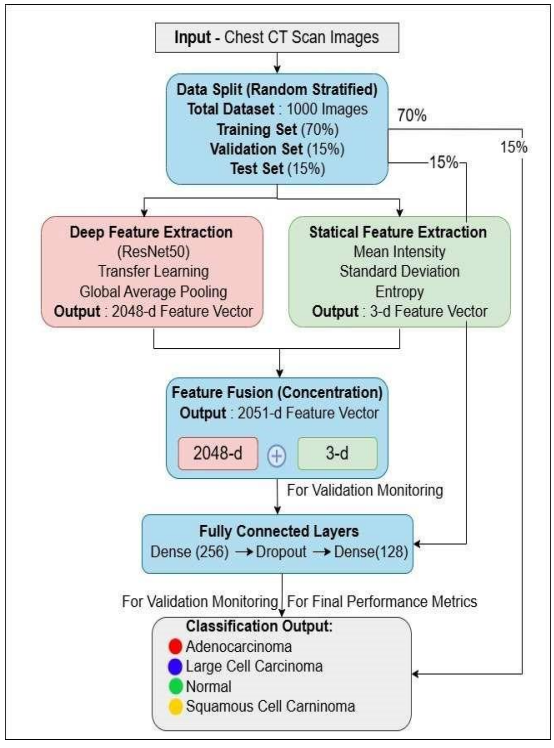

Fig. 6: Workflow of Proposed Methodology

The proposed hybrid framework extracts two complementary feature sets: F_deep represents the high-dimensional deep spatial features automatically learned by the ResNet50 backbone through the Deep Spatial Feature Extraction module. In contrast, F_quant denotes the hand-crafted quantitative features, which are manually engineered using traditional image analysis techniques such as density, texture, and other radiomic descriptors. These two feature vectors (F_deep and F_quant) are concatenated in the Hybrid Feature Fusion Layer to create a rich, multi-modal representation before passing through batch normalization and the final classifier, as shown in Figure 7. A key feature of this architecture is the two branches of feature extraction and integration.

The Deep Learning Sector (2048 features): This part is using transfer learning to implement a pre-trained deep Convolutional Neural Network (CNN) - ResNet50. The initial convolutional layers will remain frozen to retain general features that have been learnt from large databases such as ImageNet, and only fine-tune the later (deeper) convolutional layers to extract high-level spatial features within the context of lung pathology.

The Global Average Pooling layer will extract the features learned previously (Al-Sheikh et al., 2023; Azam et al., 2023).

Quantitative Feature Branch: This branch will run concurrently with the deep learning sector and will implement traditional digital image analysis of processed pixel data to generate hand-crafted quantitative features (Koo et al., 2022; Moslemi et al., 2022). The extracted quantitative features will consist of standard statistical descriptors which include Mean Intensity, Standard Deviation, and Shannon Entropy which will provide a quantitative representation of the macroscopic density (i.e., tissue density) and distribution of brightness (i.e., brightness), as well as the structural randomness of the lungs, thus providing meaningful global context that can be used to complement the spatial features extracted by the deep learning method (Moghadas-Dastjerdi et al., 2020; Moslemi et al., 2023; Walsh et al., 2024).

The two features will go through the Integration and Refinement process where the deep learning extracted spatial features as well as the hand-crafted quantitative descriptors will be combined into one complete feature vector (usually by concatenation). This combined feature representation will then go through the rest of the neural network layers to be further refined (i.e., batch norm, dropout) before being presented to the Classifier phase (Lee et al., 2025; Tada et al., 2025).

Prior to being entered into the Classifier, the combined representation will be entered into a multi-layered fully connected network to generate the final Softmax probability output for the multi-classification of Normal vs Adenocarcinoma vs Large Cell Carcinoma vs Squamous Cell Carcinoma using the same network for each class producing the probability of a class being true (George et al., 2025; Murugappan et al., 2023).

Algorithm 2 presents the training pipeline of the proposed hybrid model that combines deep CNN features with statistical features.

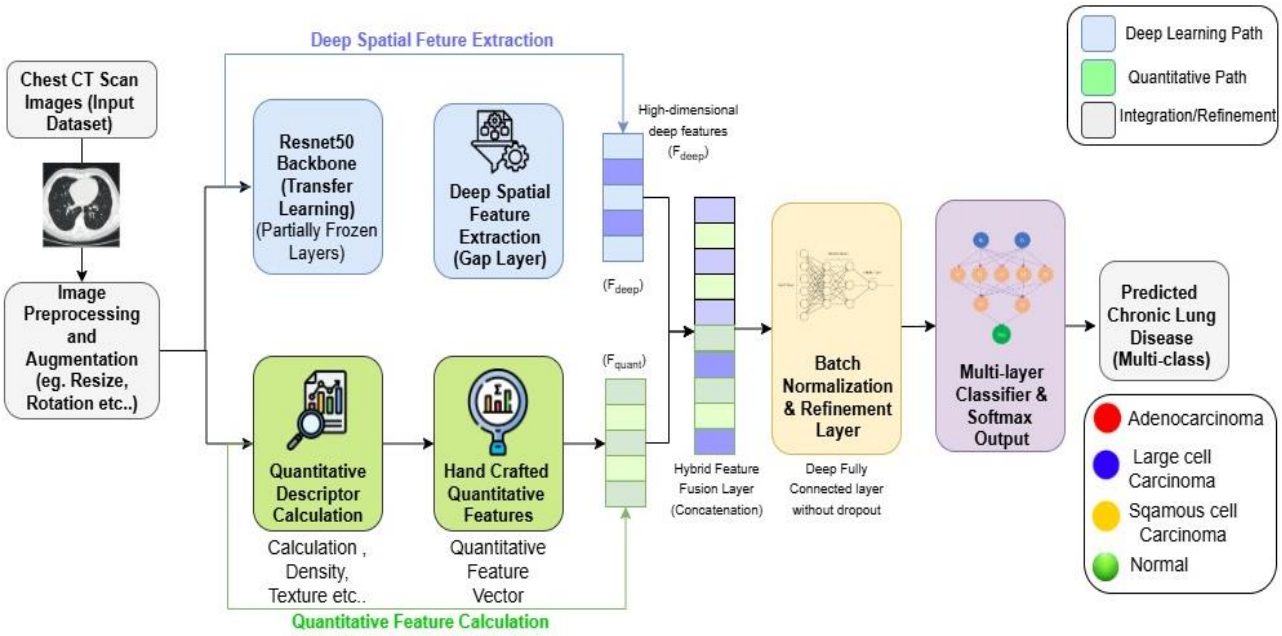

Fig. 7: Architecture of the proposed hybrid deep learning model for multi-class chronic lung disease prediction from Chest CT scan images

Table 3: Nomenclature

Symbol	Description
D = {(I, y)}	Training dataset containing input CT images (I) and corresponding labels (y)
R	Pre-trained ResNet50 backbone used for feature extraction
α	Learning rate used for model optimization
B	Batch size used during training
d	Dropout rate in the MLP classifier
E	Number of training epochs
Inorm	Pre-processed and normalized input image
$p(i)$, N	Intensity value of the i-th pixel and total number of pixels
μ	Mean pixel intensity
σ	Standard deviation of pixel intensities
H	Shannon entropy of the image
V_{stat}	Statistical feature vector $[\mu, \sigma, H]$
Fspatial/ Fdeep	Deep spatial feature vector extracted using Global Average Pooling
Ffused	Hybrid feature vector formed by concatenation
Z	Output logits from the MLP classifier
ˆ	Predicted probability distribution over classes
L	Cross-entropy loss
θ	Trainable model parameters
$\nabla_\theta L$	Gradient of loss with respect to parameters
W_1, W_2,	Weight matrices of MLP layers
b_1, b_2	Bias terms of MLP layers

In each epoch and mini-batch, it extracts statistical features (Vstat) such as mean, standard deviation, and entropy from the normalized image, and deep spatial features (Fspatial / Fdeep) using a partially frozen ResNet50 backbone with Global Average Pooling. The two feature sets are fused, passed through an MLP classifier with dropout, and the model is optimized using cross-entropy loss and the Adam optimizer. Table 3 shows the nomenclature for the algorithm.

Table 3 presents the nomenclature and description of all key symbols and mathematical notations used throughout the manuscript. This table provides a quick reference for the variables, vectors, and operators employed in the proposed hybrid model and algorithms.

Algorithm 2: Hybrid CNN–Statistical Feature Training Pipeline

Input: Training Dataset D = {(I, y)}, Pre-trained ResNet50 Backbone R,
Learning Rate α = 1e−4
Output: Optimized Hybrid Classification Model H

1: Initialization
1.1 Set hyperparameters: Batch size B = 32, Dropout rate d = 0.5, Epochs E = 25.
1.2 Initialize optimizer (Adam) and model parameters θ.

2: Pre-processing
2.1 Normalize all input images $I \in D$ to obtain I_{norm}.
2.2 Apply spatial data augmentation (rotation, flipping, zooming).

3: Model Training (Epoch-wise Optimization)
for epoch = 1 to E do
for each mini-batch $(I_{\text{norm}}, y) \in D$ do
3.1 Statistical Feature Extraction
- Compute mean: $\mu = \frac{1}{N}\sum_{i=1}^{N} P_i$
- Compute standard deviation: $\sigma = \sqrt{\frac{1}{N}\sum_{i=1}^{N}(P_i - \mu)^2}$
- Compute entropy: $H = -\sum_i p(i)\log p(i)$
- Form statistical feature vector $V_{\text{stat}} = [\mu, \sigma, H]$
3.2 Deep Spatial Feature Extraction
- Freeze initial layers of ResNet50 backbone R.
- Extract features using Global Average Pooling: $F_{\text{spatial}} = \text{GAP}(R(I_{\text{norm}}))$
3.3 Feature Fusion and Forward Pass
- Concatenate features: $F_{\text{fused}} = F_{\text{spatial}} \oplus V_{\text{stat}}$
- Pass through MLP head: $Z = W_2\big(\text{Dropout}(\text{ReLU}(W_1 F_{\text{fused}} + b_1))\big) + b_2$
- Compute predicted probabilities: $\hat{y} = \text{Softmax}(Z)$
3.4 Loss Computation and Optimization
- Compute cross-entropy loss: $L = -\sum_i y_i \log(\hat{y}_i)$
- Compute gradients: $\nabla_\theta L$
- Update parameters using Adam optimizer:
$\theta \leftarrow \theta - \alpha \cdot \nabla_\theta L$
end for
3.5 Validation and Learning Adjustment
- Evaluate model on validation set.
- If performance plateaus, reduce learning rate α.
end for

4: Model Finalization
4.1 Save trained model weights.
4.2 Return optimized model H.

Results and Discussion

We have provided a detailed analysis of the hybrid deep learning model we created to classify Chronic Lung Diseases from Computed Tomography (CT) images. The architecture of the model is multi-branch, as it uses deep transfer learning on spatial features and incorporates quantitative statistical descriptors. Novelty for our study is that we used a hybrid dataset consisting of CT images that were generated from patients after they had submitted CT scans via the Web. Evaluating the complex nature of CT images with a hybrid deep learning model presents significant challenges; however, our architecture

demonstrated exceptional results (94.00% training accuracy and 91.33% validation accuracy) after completing model development, training, and validation. Lastly, the model provided the real-world generalization and clinical relevance for the evaluation of the 15% validation dataset, with an 88.00% testing accuracy.

Training Dynamics and Convergence Strategy

In 25 epochs, the performance of the hybrid model using the training dynamics will be evaluated for consistency in learning and checking for major overfitting issues. To improve the training process, an initial rate of 10-4 was implemented using an Adam optimizer and a dynamic learning rate scheduler (ReduceLROnPlateau) was utilized based on performance (reducing the rate by one half every three epochs if no improvement occurred).

The primary convergence curves are demonstrated in Figure 8. The left plot provides the learning trajectory where the training accuracy increases sharply and eventually plateaus at 94.00% (also see point 1 below). The validation accuracy reflects the same pattern but levels out at 91.33%. The minimal gap of 0.0267 between the two final accuracies indicates how well the model fits; consequently, the model generalized well from the data, rather than simply memorizing the training set. The right plot also corroborates this finding, where both the training and validation losses decrease steadily to a minimum level with no apparent divergence, a sign of overfitting. To illustrate the peak performance of the model during this time frame, we plotted the trajectory of the model's validation accuracy separately.

As illustrated in Figure 9, the validation accuracy demonstrates a steep and efficient initial learning phase during the first 10 epochs. The learning curve then transitions into a stable refinement phase. Crucially, the model achieved its absolute peak validation performance at Epoch 20 (highlighted by the red star), reaching validation accuracy of 91.33% (also mention in Table 4). The stability of the curve in the subsequent final epochs confirms that the model successfully converged without experiencing performance degradation or overfitting, locking in highly generalizable spatial and statistical feature weights before moving to the testing phase.

Statistical Feature Relevance and EDA

Preliminary Exploratory Data Analysis (EDA) was performed on the dataset's numeric characteristics justifying the decision to use a hybrid architecture. Although deep learning provides superior performance for spatial hierarchies, classic statistical metrics allow for immediate global context (Huang et al., 2017).

Applying pixel intensity distribution analysis and statistical feature heat maps demonstrated significant differences between classes. For example, Shannon entropy and pixel intensity standard deviation values were significantly different when comparing healthy tissue to Large Cell Carcinoma and Squamous Cell Carcinoma, which are denser and more disordered tissues. Global descriptors (mean intensity, standard deviation and entropy) have been incorporated into the second branch of the hybrid architecture to compel the model to combine macroscopic tissue density, with the microscopic spatial characteristics as learned by the ResNet50 architecture (Lanjewar et al., 2023; Muthuchamy and Preethika, 2025).

Table 4: Summary of Model Training and validation

Dataset Phase	Data Split	Total Images	Overall Accuracy
Training	70%	700	94.00%
Validation	15%	150	91.33%

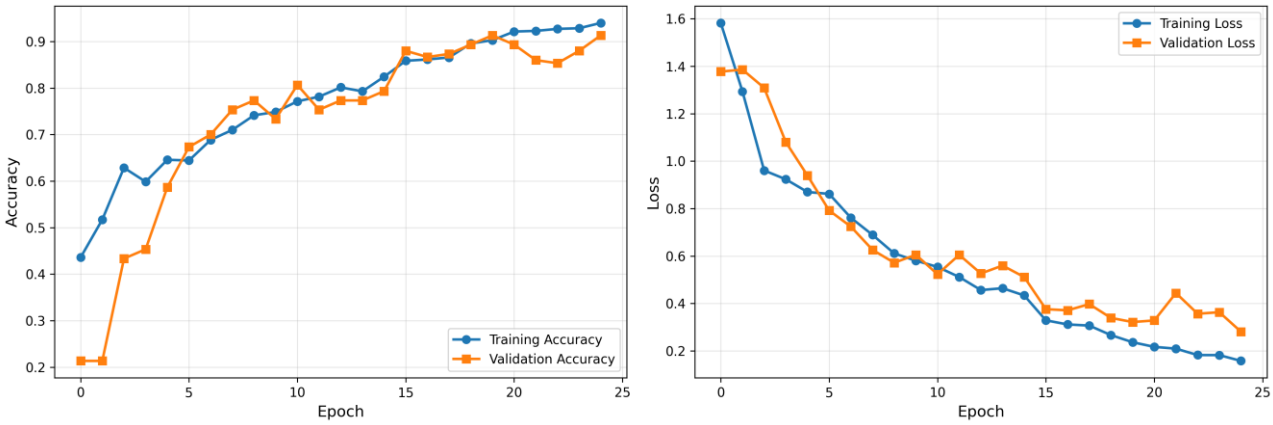

Fig. 8: Training and Validation Accuracy/Loss History over 25 Epochs

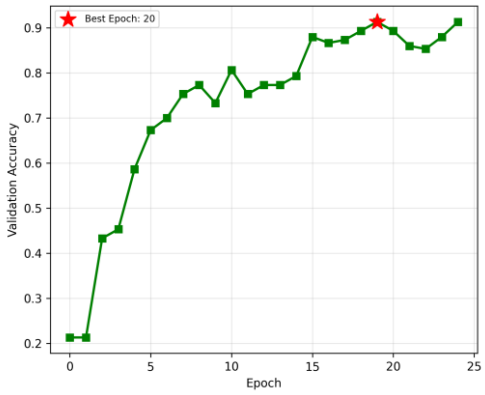

Fig. 9: Isolated Validation accuracy in 20 epochs

Comprehensive Evaluation on 15% Testing Dataset

The model was rigorously evaluated after its training on an independent 15% (150 images) test data set to assess its diagnostic reliability in simulated clinical settings.

Table 5 presents the comprehensive performance metrics of the proposed hybrid model on the 15% test dataset. An overall accuracy of 88.00% on unseen medical imaging data is an impressive result for the model. The model exhibited strong performance for the identification of the "Normal" tissue class, with precision and recall values both at 0.9688 being close to perfect accuracy. Additionally, a weighted average F1-Score of 0.8796 shows the model maintained high-quality diagnostic performance across specific classes of cancer despite having high levels of class imbalance. To visually validate the parity and balance of these predictive capabilities across the distinct classes, we mapped the core metrics onto a performance radar chart.

A multi-dimensional representation of the model's robustness is shown in Figure 10. Since Precision (blue), Recall (red), and F1-Score (green) lines form a nearly symmetrical, expansive diamond shape, it is indicated that the model is not highly biased towards any one of the majority classes. The "Normal" class does show some slight bias; however, it is clustered very tightly near the 1.0 cutoff point, indicating that healthy tissues are classified very well. The model performs consistently across Adenocarcinoma, Large Cell Carcinoma, and Squamous Cell Carcinoma, which confirms that the weighted average F1-Score value of 0.8796 accurately represents how uniformly well the model will make diagnoses of each of the classes, rather than significantly increasing due to a single class with a significantly higher value than all other classes combined (i.e. the Normal class).

Ablation Study

To validate the contribution of the proposed hybrid architecture, we performed an ablation study by comparing the performance of the integrated ResNet50-MLP framework against its individual components. The models were evaluated using the same patient-level data split and experimental conditions. The standalone ResNet50 architecture achieved a testing accuracy of 84%. Incorporating statistically determined measures via the MLP branch improved the overall classification accuracy to 85.0%. This comparison demonstrates that the hybrid approach provides a more robust feature representation by merging high-level spatial properties with specific intensity-based diagnostic markers, ultimately enhancing the model's discriminative power.

Class Discrimination and Misclassification

To gain insight into the limitations of the classifier, we performed a deep-dive into the classifier's exact prediction distributions with a confusion matrix as shown in Figure 11. The model misidentified only 18 of the 150 test images.

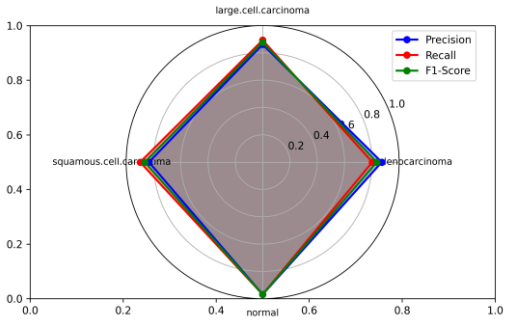

Fig. 10: Performance Radar Chart

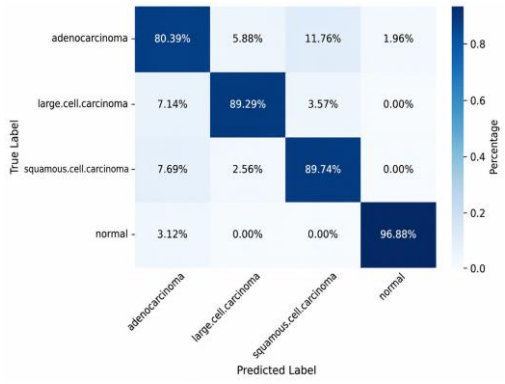

Fig. 11: Confusion Matrix (Normalized by True Label) for 4-Class Test Predictions

Table 5: Comprehensive Model Performance Metrics (15% Test Dataset)

Class Label	Precision	Recall	F1-Score	Support
Adenocarcinoma	0.8723	0.8039	0.8367	51
Large Cell Carcinoma	0.8621	0.8929	0.8772	28
Squamous Cell Carcinoma	0.8333	0.8974	0.8642	39
Normal (Healthy)	0.9688	0.9688	0.9688	32

Therefore, the overall misclassification error rate for the model is a low 12.0%. From an architectural standpoint, the visual similarity led to highly overlapping global statistical descriptors (such as mean intensity and entropy) in these edge cases, limiting the Multi-Layer Perceptron's (MLP) ability to establish a definitive mathematical boundary.

The quantitative analysis indicates specific diagnostic challenges consistent with known clinical difficulties. The class Adenocarcinoma had the most instances (6 total) where misclassified as Squamous Cell Carcinoma (11.8% of all errors). Three Adenocarcinomas were also misclassified as Large Cell Carcinomas. Furthermore, three Squamous Cell Carcinomas were also misclassified as Adenocarcinomas. This overlap is clinically expected because when looking at CT images, there are very few clear morphological and textural differences between these two subtypes of non-small-cell lung carcinoma, even for human radiologists, there often aren't definitive borders separating these two subtypes in CT imaging. Additionally, the confusion between cancerous classes and normal scans remains low (only one normal scan was misclassified as Adenocarcinoma), indicating that the model is reliable when used as an initial screening tool. This low false-positive rate indicates that the hybrid model is reliable when utilized as an initial resource-efficient screening and triaging tool. To assess the model's ability to discriminate, we used Receiver Operating Characteristic (ROC) curves and area under curve (AUC) scores across all decision thresholds.

ROC curve results, plotted using an OvR (one vs. rest) approach, are shown in Figure 12. The model classifies all of the classes as strictly falling within this highest-level classification. The model has a perfect AUC of 1.000 for the normal tissue class, while, among the malignant tissue classes, the large cell carcinoma (LCC) class has an AUC of 0.984, squamous cell carcinoma (SCC) has an AUC of 0.962, and adenocarcinoma has an AUC of 0.950. The hybrid model also has a micro-average AUC of 0.9755, which indicates that it has an outstanding ability to discriminate.

Model Interpretability and Visual Explanation

In order to further provide evidence for the clinical reliability of the indicative hybrid framework and to counteract the inherent uncertainty created by deep learning "black box" classifiers when interpreting their results, Explainable AI (XAI) methods were incorporated into the evaluation process of this study. Figure 13 depicts an example of a visual interpretability analysis of a CT scan that was correctly classified by the proposed method. The analysis was completed using either Gradient Saliency Mapping or Local Interpretable.

Explainable AI (XAI) Visualizations: The top row displays the Original CT scan, Gradient Saliency Overlay, and Saliency Heatmap. Bottom row displays the LIME Superpixel Overlay and the isolated Positive Features driving the model's prediction.

Model-agnostic Explanations (LIME) techniques: The top row of the figure is composed of the Gradient Saliency Overlay image and its associated Heat map image showing pixel-level intensity gradients that contributed most prominently to the activation of ResNet50's spatial branch. The bottom portion of the figure is composed of images resulting from the use of LIME to segment the anatomical structures into superpixels and produce the Positive Features map indicating which anatomical structures provide the morphological features of interest and ultimately support the classification decision. Collectively, these visualizations demonstrate that the predictive accuracy of the model for diagnosing disease is based on relevant pathophysiologic and anatomic elements of the lung rather than extraneous background artifacts. As a result, the availability of this type of visual interpretation of the classification process will significantly improve collaborative diagnostic transparency and ultimately foster greater collaborative trust in the radiologist-physician diagnosis of lung disease.

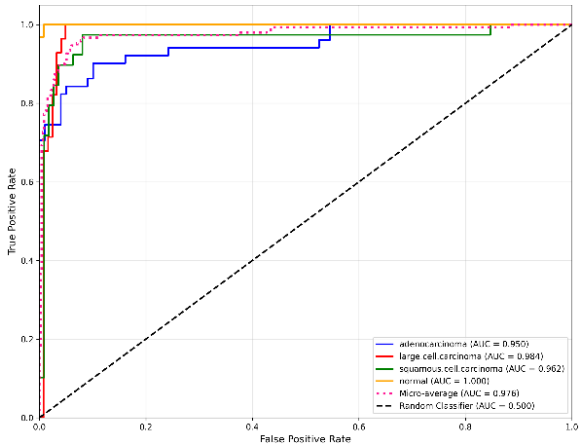

Fig. 12: Multi-Class One-vs-Rest ROC Curves and AUC Scores

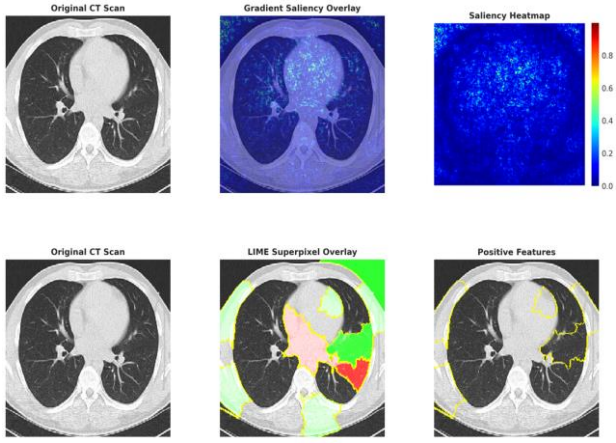

Fig. 13: Explainable AI (XAI) Comparative Visualization

Based on a comparison with other methods listed in Table 1, the proposed hybrid deep learning model has significantly better performance and robustness. Most studies on single architecture deep learning methods (e.g., CNN, transformer, attention mechanism) have had moderately considerable accuracy results. They focus on a detection task, have complicated multiple processing pipelines, and do not have complete integration of features, rendering them less effective for multi-class classification. The overwhelming majority of deep learning models being used today were trained on only a small number of limited diverse datasets from CT machines. This training has led to several problems: Overfitting, decreased generalization capability and a lack of robustness when applied to clinical situations in the real world. Our proposed method combines statistical features extracted from CT images with deep spatial information extracted from CT images. This hybrid feature fusion directly addresses gaps found within related literature. These hybrid features lead to significantly improved overall performance of a machine learning classifier. By achieving 94% training accuracy, 91.33% validation accuracy and 88% testing accuracy (on unseen data), our hybrid classifier demonstrated an ability to generalize results well. The small difference between training and validation accuracies lends additional support to the conclusion that our method can classify lung diseases more effectively than single classifiers have previously demonstrated. Therefore, we can conclude that our method not only outperforms other single branch and partially hybrid models but also provides a more scalable solution for clinically classifying lung diseases.

Conclusion

We developed and rigorously evaluated an innovative hybrid deep learning model that addresses important deficiencies found in most existing CADs for chronic lung disease. This study utilizes a recently compiled, highly quantitative set of chest CT examinations to resolve the issues of clinical relevance and generalizability typically associated with older, heavily saturated publicly available benchmark dataset. We also create a framework to move from single modality architectures to a dual modality combination by using a dual feature integration approach. Specifically, we use a fine-tuned ResNet50 backbone to extract detailed high-level spatial hierarchies of the lungs while simultaneously combining them with globally representative statistical descriptors (mean intensity, standard deviation, and entropy). With the multi-branch approach, the model is able to capture both localized structural deterioration as well as broad macroscopic tissue density, which are two types of pathological signatures that conventional networks based entirely on image data consistently cannot quantify.

The research filled the gap in the literature on multi-class fine-grained classification by developing a framework that spanned multiple disciplines and utilized a novel hybrid method. The research results were noteworthy for successfully implementing a hybrid approach while maintaining computational constraints by freezing the majority of the deep network's layers in the long term and using a lightweight MLP to maximize predictive modelling performance with less use of expensive GPUS. Under the most optimal configurations for the hybrid system, the hybrid system exceeded the previous plateau of 87 to 93% performance established by prior research and achieved an excellent training accuracy of 94.00% and validation accuracy of 91.33% %.

Moreover, the model's ability to generalize to real-world data was also shown to be remarkable, as it achieved a testing accuracy of 88.00% and exhibited the ability (Micro-average AUC = 0.9755) for the four diagnostic classes tested. These outcomes provide definitive support for the large potential of hybrid feature integration implemented in a resource efficient manner. This platform combines deep spatial latent representations with handcrafted global statistics to create a highly reliable and scalable foundation for the future development of CAD tools in the area of pulmonary oncologic imaging. Even though the hybrid architecture has the same degree of balanced classification performance as the existing methods, we will need additional comparative experiments with simpler baseline models to quantify the impact of the statistical feature branch on performance. The current study lacks external validation and multi-center evaluation, which are essential for future generalization. In future studies, we will expand our study of this hybrid architecture to larger and more diverse multi-institutional data sets to improve generalizability and clinical reliability of the model.

Acknowledgment

We express our profound gratitude for the accessibility to scholarly resources and institutional facilities afforded by Sir Padampat Singhania University, which significantly facilitated the fulfillment of this research endeavor.

Funding Information

This research did not receive any funding.

Author’s Contributions

Garima Jain: Conceptualization, proposal methodology, analysis, and original draft writing.

Amit Kumar Goel and Rahul Kumar: Review and Edited.

Ethics

This manuscript is an original work. The authors declare that there are no ethical concerns associated with this submission.

References

Abdulqader, A. F., Abdulameer, S., Bishoyi, A. K., Yadav, A., Rekha, M. M., Kundlas, M., Kavitha, V., Aminov, Z., Abdulali, Z. S., Alwan, M., Jawad, M., Mushtaq, H., & Farhood, B. (2025). Multi-objective deep learning for lung cancer detection in CT images: enhancements in tumor classification, localization, and diagnostic efficiency. *Discover Oncology*, *16*(1), 529. https://doi.org/10.1007/s12672-025-02314-8

Alsallal, M., Ahmed, H. H., Kareem, R. A., Yadav, A., Ganesan, S., Shankhyan, A., Gupta, S., Joshi, K. K., Sameer, H. N., Yaseen, A., Athab, Z. H., Adil, M., & Farhood, B. (2025). Enhanced lung cancer subtype classification using attention-integrated DeepCNN and radiomic features from CT images: a focus on feature reproducibility. *Discover Oncology*, *16*(1), 336. https://doi.org/10.1007/s12672-025-02115-z

Al-Sheikh, M. H., Al Dandan, O., Al-Shamayleh, A. S., Jalab, H. A., & Ibrahim, R. W. (2023). Multi-class deep learning architecture for classifying lung diseases from chest X-Ray and CT images. *Scientific Reports*, *13*(1), 1–14. https://doi.org/10.1038/s41598-023-46147-3

Azam, S., Rafid, A. K. M. R. H., Montaha, S., Karim, A., Jonkman, M., & Boer, F. D. (2023). Automated Detection of Broncho-Arterial Pairs Using CT Scans Employing Different Approaches to Classify Lung Diseases. *Biomedicines*, *11*(1), 133. https://doi.org/10.3390/biomedicines11010133

Baqir, M. A., Qayyum, S., Ashfaq, N., Li, J., Wang, Y., Mahmood, T., & Saba, T. (2026). A lightweight CNN for enhanced non-small cell lung cancer classification using CT scan image. *Scientific Reports*, *16*(1), 12985. https://doi.org/10.1038/s41598-026-41401-w

Bhattacharjya, U., Sarma, K. K., Kakati, A., Medhi, J. P., Barman, G., & Choudhury, B. K. (2025). Attention-Driven Enhancements in YOLOv8s for Improved Detection of Respiratory Conditions From HRCT Scans. *IEEE Sensors Letters*, *9*(7), 1–4. https://doi.org/10.1109/lsens.2025.3576896

Choudhury, A. R., Rautray, J., Mishra, P., Kandpal, M., & Dalai, S. S. (2025). Deep Learning Based Automated Lung Cancer Detection from CT scan Leveraging Transfer Learning. *Procedia Computer Science*, *258*, 2748–2759. https://doi.org/10.1016/j.procs.2025.04.535

Córdoba, I. H. de, Mielgo-Rubio, X., Cejas, P., Ramos, J. P., Garrido-Rubiales, B., Martínez, S. F., Romero, G. R., Parga, M. M., Taltavull, L. M., González, A. F., Sáenz, E. C., & Sereno, M. (2025). Transformation to Neuroendocrine Phenotype in Non-Small-Cell Lung Carcinoma: A Literature Review. *International Journal of Molecular Sciences*, *26*(11), 5096. https://doi.org/10.3390/ijms26115096

Davri, A., Birbas, E., Kanavos, T., Ntritsos, G., Giannakeas, N., Tzallas, A. T., & Batistatou, A. (2023). Deep Learning for Lung Cancer Diagnosis, Prognosis and Prediction Using Histological and Cytological Images: A Systematic Review. *Cancers*, *15*(15), 3981. https://doi.org/10.3390/cancers15153981

Faizi, M. K., Qiang, Y., Wei, Y., Qiao, Y., Zhao, J., Aftab, R., & Urrehman, Z. (2025). Deep learning-based lung cancer classification of CT images. *BMC Cancer*, *25*(1), 1–13. https://doi.org/10.1186/s12885-025-14320-8

Forte, G. C., Altmayer, S., Silva, R. F., Stefani, M. T., Libermann, L. L., Cavion, C. C., Youssef, A., Forghani, R., King, J., Mohamed, T.-L., Andrade, R. G. F., & Hochhegger, B. (2022). Deep Learning Algorithms for Diagnosis of Lung Cancer: A Systematic Review and Meta-Analysis. *Cancers*, *14*(16), 3856. https://doi.org/10.3390/cancers14163856

George, A. B., George, S. J. R. A. B., & Sreehari, J.R. (2025). *Multi-Modal Oral Cancer Detection Using Weighted Ensemble Convolutional Neural Networks*. https://doi.org/10.48550/arXiv.2510.03878

Gote, P. M., Kumar, P., Kumar, H., Verma, P., & Jiet, M. M. (2025). Integrating Machine Learning Algorithms: A Hybrid Model for Lung Cancer Outcome Improvement. *Applied Sciences*, *15*(9), 4637. https://doi.org/10.3390/app15094637

Hosny, M., Elgendy, I. A., & Albashrawi, M. A. (2025). Multi-Modal Deep Learning for Lung Cancer Detection Using Attention-Based Inception-ResNet. *IEEE Access*, *13*, 123630–123648. https://doi.org/10.1109/access.2025.3588407

Huang, G., Liu, Z., Van Der Maaten, L., & Weinberger, K. Q. (2017). Densely Connected Convolutional Networks. *Proceedings of the IEEE Conference on Computer Vision and Pattern Recognition*, 4700–4708. https://doi.org/10.1109/cvpr.2017.243

Huang, K. A., Venkitasubramony, V., & Prakash, N. S. (2025). Leveraging Transfer Learning and Attention Mechanisms for a Computed Tomography Lung Cancer Classification Model. *Cureus*, *17*(6), e87071. https://doi.org/10.7759/cureus.87071

Ichahane, M. Y., Assad, N., & Ouahmane, H. (2026). Enhancing Rheumatoid Arthritis Diagnosis: Combining Case-Based Reasoning on EHR Data with Deep Learning on Medical Images *JUCS - Journal of Universal Computer Science*, *32*(3), 373–404. https://doi.org/10.3897/jucs.130529

Inbasakaran, G., & Ruth, J. A. (2025). Clinical-ready CNN framework for lung cancer classification: Systematic optimization for healthcare deployment with enhanced computational efficiency. *Intelligence-Based Medicine*, *12*, 100292. https://doi.org/10.1016/j.ibmed.2025.100292

Jain, R. K., Hiran, K. K., Maheshwari, R., & Vaishali. (2023). Lung Cancer Detection Using Machine Learning Algorithms. *2023 International Conference on Computational Intelligence, Communication Technology and Networking (CICTN)*, 516–521. https://doi.org/10.1109/cictn57981.2023.10141467

Javed, R., Abbas, T., Khan, A. H., Daud, A., Bukhari, A., & Alharbey, R. (2024). Deep learning for lungs cancer detection: a review. *Artificial Intelligence Review*, *57*(8), 197. https://doi.org/10.1007/s10462-024-10807-1

Kamala, L., & Mohan, K. G. (2025). An efficient hybrid artificial intelligence framework for lung cancer classification using CT images. *Scientific Reports*, *16*(1), 1777. https://doi.org/10.1038/s41598-025-31432-0

Khan, K., & Aleem, A. (2025). A Hybrid Approach Combining YOLO and Deep Neural Networks for Efficient Lung Disease Detection. *2025 3rd International Conference on Communication, Security, and Artificial Intelligence (ICCSAI)*, 1204–1211. https://doi.org/10.1109/iccsai64074.2025.11064147

Khan, S., Noor, M. N., Ashraf, I., Masud, M. I., & Aman, M. (2026). Impact of CT Intensity and Contrast Variability on Deep-Learning-Based Lung-Nodule Detection: A Systematic Review of Preprocessing and Harmonization Strategies (2020–2025). *Diagnostics*, *16*(2), 201. https://doi.org/10.3390/diagnostics16020201

Kobylińska, K., Orłowski, T., Adamek, M., & Biecek, P. (2022). Explainable Machine Learning for Lung Cancer Screening Models. *Applied Sciences*, *12*(4), 1926. https://doi.org/10.3390/app12041926

Koo, C. W., Williams, J. M., Liu, G., Panda, A., Patel, P. P., Frota Lima, L. M. M., Karwoski, R. A., Moua, T., Larson, N. B., & Bratt, A. (2022). Quantitative CT and machine learning classification of fibrotic interstitial lung diseases. *European Radiology*, *32*(12), 8152–8161. https://doi.org/10.1007/s00330-022-08875-4

Lanjewar, M. G., Panchbhai, K. G., & Charanarur, P. (2023). Lung cancer detection from CT scans using modified DenseNet with feature selection methods and ML classifiers. *Expert Systems with Applications*, *224*, 119961. https://doi.org/10.1016/j.eswa.2023.119961

Lee, J., Kim, M., Park, H., Yang, Z., Woo, O. H., Kang, W. Y., & Kim, J. H. (2025). Enhanced Detection Performance of Acute Vertebral Compression Fractures Using a Hybrid Deep Learning and Traditional Quantitative Measurement Approach: Beyond the Limitations of Genant Classification. *Bioengineering*, *12*(1), 64. https://doi.org/10.3390/bioengineering12010064

Makimoto, K., Virdee, S., Koo, M., Hogg, J. C., Bourbeau, J., Tan, W. C., & Kirby, M. (2025). Upper-lobe CT imaging features improve prediction of lung function decline in COPD. *ERJ Open Research*, *11*(3), 00876–02024. https://doi.org/10.1183/23120541.00876-2024

Mijwil, M. M., Aggarwal, K., Doshi, R., Hiran, K. K., & Sundaravadivazhagan, B. (2022). Deep Learning Techniques for COVID-19 Detection Based on Chest X-ray and CT-scan Images: A Short Review and Future Perspective. *Asian Journal of Applied Sciences*, *10*(3), 2321–0893. https://doi.org/10.24203/ajas.v10i3.6998

Moghadas-Dastjerdi, H., Sha-E-Tallat, H. R., Sannachi, L., Sadeghi-Naini, A., & Czarnota, G. J. (2020). A priori prediction of tumour response to neoadjuvant chemotherapy in breast cancer patients using quantitative CT and machine learning. *Scientific Reports*, *10*(1), 10936. https://doi.org/10.1038/s41598-020-67823-8

Moslemi, A., Kontogianni, K., Brock, J., Wood, S., Herth, F., & Kirby, M. (2022). Differentiating COPD and asthma using quantitative CT imaging and machine learning. *European Respiratory Journal*, *60*(3), 2103078. https://doi.org/10.1183/13993003.03078-2021

Moslemi, A., Makimoto, K., Tan, W. C., Bourbeau, J., Hogg, J. C., Coxson, H. O., & Kirby, M. (2023). Quantitative CT Lung Imaging and Machine Learning Improves Prediction of Emergency Room Visits and Hospitalizations in COPD. *Academic Radiology*, *30*(4), 707–716. https://doi.org/10.1016/j.acra.2022.05.009

Murugappan, M., Bourisly, A. K., Prakash, N. B., Sumithra, M. G., & Acharya, U. R. (2023). Automated semantic lung segmentation in chest CT images using deep neural network. *Neural Computing and Applications*, *35*(21), 15343–15364. https://doi.org/10.1007/s00521-023-08407-1

Muthuchamy, K., & Preethika, S. K. P. (2025). Deep Learning in Oncology: Improving Early Cancer Detection with UNet, EfficientNet, and DenseNet. *2025 9th International Conference on Inventive Systems and Control (ICISC)*, 231–236. https://doi.org/10.1109/icisc65841.2025.11188005

Nahmatwlla, L. L., & Ali, A. M. (2026). ResNet-SEMultiRes: A Deep Learning Framework for Primary Lung Cancer Classification Using CT Scan Image. *Indian Journal of Radiology and Imaging*, *36*(3), 289–441. https://doi.org/10.1055/s-0045-1815732

Purohit, P., Goswami, C., & Hiran, K. K. (2025). Fusion of Hybrid AI and Dynamic Multi-Layered Feature Learning for Precision Driven Cardiovascular Disease Diagnosis. *Journal of Innovative Image Processing*, *7*(2), 476–503. https://doi.org/10.36548/jiip.2025.2.010

Raghu, A., Raghu, A., & Wise, J. F. (2024). Deep Learning–Based Identification of Tissue of Origin for Carcinomas of Unknown Primary Using MicroRNA Expression: Algorithm Development and Validation. *JMIR Bioinformatics and Biotechnology*, *5*, e56538. https://doi.org/10.2196/56538

Ramasamy, J., & Doshi, R. (2022). Machine Learning in Cyber Physical Systems for Healthcare. *Real-Time Applications of Machine Learning in Cyber-Physical Systems*, 65–76. https://doi.org/10.4018/978-1-7998-9308-0.ch005

Şerbănescu, M.-S., Oancea, C.-N., Streba, C. T., Pleşea, I. E., Pirici, D., Streba, L., & Pleşea, R. M. (2020). Agreement of two pre-trained deep-learning neural networks built with transfer learning with six pathologists on 6000 patches of prostate cancer from Gleason2019 Challenge. *Romanian Journal of Morphology and Embryology*, *61*(2), 513–519. https://doi.org/10.47162/rjme.61.2.21

Shafi, S. M., & Chinnappan, S. K. (2024). Hybrid transformer-CNN and LSTM model for lung disease segmentation and classification. *PeerJ Computer Science*, *10*, e2444. https://doi.org/10.7717/peerj-cs.2444

Shatnawi, M. Q., Abuein, Q., & Al-Quraan, R. (2025). Deep learning-based approach to diagnose lung cancer using CT-scan images. *Intelligence-Based Medicine*, *11*, 100188. https://doi.org/10.1016/j.ibmed.2024.100188

Sing, T., Hoefling, H., Hossain, I., Boisclair, J., Doelemeyer, A., Flandre, T., Piaia, A., Romanet, V., Santarossa, G., Saravanan, C., Sutter, E., Turner, O., Wuersch, K., & Moulin, P. (2019). A deep learning-based model of normal histology. *BioRxiv*. https://doi.org/10.1101/838417

Soni, A., & Rai, A. (2023). An Efficient CNN Model for Automatic Diagnosis of Cardiomegaly from Chest Radiographic Images. *International Journal of Image, Graphics and Signal Processing*, *15*(3), 81–96. https://doi.org/10.5815/ijigsp.2023.03.07

Sui, H., Mo, Z., Wei, Y., Shi, F., Cheng, K., & Liu, L. (2025). Diagnosis and Severity Assessment of COPD Based on Machine Learning of Chest CT Images. *International Journal of Chronic Obstructive Pulmonary Disease*, *Volume 20*, 2853–2867. https://doi.org/10.2147/copd.s528988

Sun, J., Liao, X., Yan, Y., Zhang, X., Sun, J., Tan, W., Liu, B., Wu, J., Guo, Q., Gao, S., Li, Z., Wang, K., & Li, Q. (2022). Detection and staging of chronic obstructive pulmonary disease using a computed tomography–based weakly supervised deep learning approach. *European Radiology*, *32*(8), 5319–5329. https://doi.org/10.1007/s00330-022-08632-7

Tada, D. K., Kim, G. H., Goldin, J. G., Teng, P., Vyapari, K., Banola, A., Abtin, F., McNitt-Gray, M., & Brown, M. S. (2025). Using a fully automated, quantitative fissure integrity score extracted from chest CT scans of emphysema patients to predict endobronchial valve response. *Journal of Medical Imaging*, *12*(02), 024501. https://doi.org/10.1117/1.jmi.12.2.024501

Tone, M., Isono, T., Yamamoto, Y., Takeda, Y., Shintani, Y., Kumanogoh, A., Wada, H., & Iwahori, K. (2025). Lung tissue T cells are activated in chronic obstructive pulmonary disease with non-small cell lung cancer patients. *Scientific Reports*, *15*(1), 41209. https://doi.org/10.1038/s41598-025-25141-x

UrRehman, Z., Qiang, Y., Wang, L., Shi, Y., Yang, Q., Khattak, S. U., Aftab, R., & Zhao, J. (2024). Effective lung nodule detection using deep CNN with dual attention mechanisms. *Scientific Reports*, *14*(1), 3934. https://doi.org/10.1038/s41598-024-51833-x

Walsh, S. L. F., Backer, J. D., Prosch, H., Langs, G., Calandriello, L., Cottin, V., Brown, K. K., Inoue, Y., Tzilas, V., & Estes, E. (2024). Towards the adoption of quantitative computed tomography in the management of interstitial lung disease. *European Respiratory Review*, *33*(171), 230055. https://doi.org/10.1183/16000617.0055-2023

Zaernia, A., Youseffi, M., Parisi, L., Abd-Alhameed, R., & Ma, R. (2024). A Novel Artificial Intelligence-Driven Technique for Enhancing Medical Imaging Techniques to Detect Non-Small Cell Lung Cancer. *2024 12th European Workshop on Visual Information Processing (EUVIP)*, 1–6. https://doi.org/10.1109/euvip61797.2024.10772826